Highly Sensitive Air-Gap Fiber Fabry–Pérot Interferometers Based on Polymer-Filled Hollow Core Fibers

Cheng-Ling Lee, Lin-Hung Lee, Hone-Ene Hwang, and Jui-Ming Hsu

***Abstract*— This letter, for the first time, investigates a novel, and ultracompact air-gap fiber Fabry–Pérot interferometer (AG-FFPI), which is based on a polymer-filled hollow core fiber (HCF) endface. The proposed polymer-filled AG-FFPI has advantages of easy fabrication, high temperature sensitivity, low cost, and arbitrary length of air-gap. The variation of the Fabry–Pérot cavity length can be greatly enhanced from exploiting the high thermal expansion coefficient of the elastic polymer-filled in the HCF. The proposed device exhibits a wavelength shift of the interference fringes that corresponds to temperature sensitivity of −1.7 nm/°C, which is equivalent to sensitivity to a change in cavity length of −21.9nm/°C.**

***Index Terms*— Air-gap fiber Fabry–Pérot interferometer (AG-FFPI), fiber optics component, fiber sensors, hollow core fiber (HCF), polymer.**

I. Introduction

THE IN-LINE air-gap fiber Fabry–Pérot interferometer (AG-FFPI) simply utilizes two reflections of optical light reflected by the first and second fiber/air interfaces to generate low-finesse interference fringes. It is used in a wide range of practical applications, and especially in sensing applications. Varieties configurations of the AG-FFPIs have been developed with numerous smart and hybrid structures to perform different physical sensing measurements [1]–[10]. The AG-FFPIs are typically fabricated by precisely aligning two fiber endfaces [1]–[3] to form an extrinsic type AG-FFPI. Another technique involves use of fs-laser micromachining to carve the fiber to form the air-gap. This method is advanced, convenient and requires no alignment, but it does require an expansive laser [4]–[5]. The formation of compact and intrinsic AG-FFPIs by using etching and splicing processes to form the air-gap of a certain distance as an F-P cavity has been presented [6]–[7]. The device thus formed can be adapted to sense temperature (T) and strain (ε). We have presented a novel, simple, cost- effective and sensitive AG-FFPI that is formed by overlaying the endface of a fiber metallic tin (Sn) around [8]. The air-gap was formed between the surface of the Sn and end of the fiber. The high thermal expansion coefficient (TEC) of Sn ($\sim 2.2 \times 10^{-5}$ °C^{-1}), which is 40 times that of the silica fiber ($\sim 5.5 \times 10^{-7}$ °C^{-1}), enables a very high T sensitivity to be obtained [8].

Manuscript received September 2, 2011; revised October 22, 2011; accepted October 28, 2011. Date of publication November 2, 2011; date of current version January 6, 2012. This work was supported in part by the National Science Council of the Republic of China under Grant NSC 98-2221-E-239-002-MY2.

C.-L. Lee, L.-H. Lee, and J.-M. Hsu are with the Department of Electro-Optical Engineering, National United University, Miaoli 360, Taiwan (e-mail: cherry@nuu.edu.tw; gn01140216@hotmail.com; jmhsu@nuu.edu.tw).

H.-E. Hwang is with the Department of Electronic Engineering, Chung Chou Institute of Technology, Yuanlin 510, Taiwan (e-mail: n741@ms26.hinet.net).

Color versions of one or more of the figures in this letter are available online at http://ieeexplore.ieee.org.

Digital Object Identifier 10.1109/LPT.2011.2174632

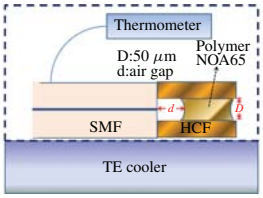

Fig. 1. Configuration of proposed polymer-filled AG-FFPI.

Other smart configurations of AG-PPFIs, such as splicing an air bubble skillfully between the fiber and a photonic crystal fiber (PCF) [9] and splicing a section of a hollow core fiber (HCF) [10], are reportedly effective in the fabrication of air-gap Fabry–Pérot cavities.

This Letter presents for the first time a very simple, ultracompact and highly sensitive, polymer-filled air-gap fiber Fabry–Pérot interferometer (AG-FFPI) for sensing temperature (T). The proposed sensor is composed of a single mode fiber (SMF) splicing a hollow-cored fiber (HCF). The endface of HCF is filled with a section of the monomer and kept an air-gap remained between the SMF and the monomer (Fig. 1). The length of the air-gap can be easily controlled by varying the duration of filling by capillary action. The monomer, Norland Optical Adhesive 65 (NOA65), is a photo-polymerizable liquid that can be cured by ultraviolet (UV) light with a maximum absorption in the range 350–380 nm. The monomer can be formed as a solid polymer structure by the UV exposing process. The solid edge of the polymer wall can fix the air-gap structure of the device and make the width of the air-gap permanent. Fig. 1 presents the proposed AG-FFPI device. Many polymer-filled AG-FFPIs with several widths of air-gaps are fabricated and further applied to measure the surrounding T. Experimental results demonstrate that greatly variation of the Fabry–Pérot cavity length as well as highly sensitive property of the sensors can be obtained by the high thermal expansion coefficient of the polymer.

II. Polymer-Filled AG-FFPI Sensor Configuration and Principle of Operation

In the experiment, the SMFs were firstly spliced different lengths of HCFs by using a special fusion method. Then,

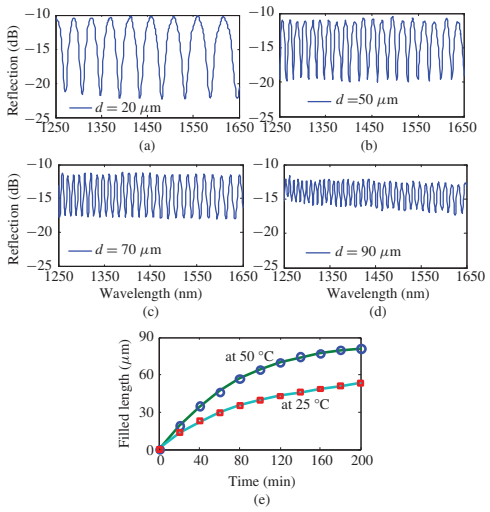

Fig. 2. Experimental reflection spectra of proposed device with air-gap d of (a) 20 μm, (b) 50 μm, (c) 70 μm, (d) 90 μm, and (e) filled length of NOA65 as a function of the duration of capillary action at different T.

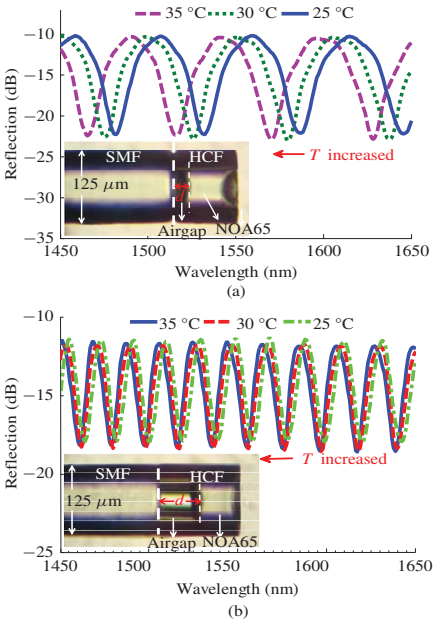

Fig. 3. Interference spectra of proposed device with air-gap (a) $d \sim 20$ μm and (b) $d \sim 70$ μm as surrounding T varies. Insets show micrographs of endface structure.

the endface of the HCFs was filled with monomer NOA65 for the duration of the capillary action to ensure that the same quantity of monomer in the core of the HCFs. Thus, different empty lengths, full of air, remained in the front sections of the HCFs. The filled lengths and the quantity of the monomer NOA65 were controlled by varying the duration of the capillary action. In this work, the polymer-filled length was around 70 μm, but larger lengths of 200 $\sim$ 300 μm can also be performed based on our experience. After filling, the endface of HCF was exposed to UV light with an intensity of approximately 10 mW/cm^2 for 6hr at room temperature. In the UV-curing process, the monomer NOA65 with a refractive index of about 1.515 gradually transformed into solid polymer with an refractive index of 1.524; solid walls of the polymer NOA65 were established and one of the wall which acts as the mirror of the Fabry–Pérot (F-P) interferomtric cavity. The thermophysical and thermomechanical properties of the UV-cured NOA65 may change with the different curing processes used [11]. Based on the authors' experience, the intensity and duration of exposure can be controlled to turn the monomer into a hard solid to stabilize the width of the air-gap. Since the UV-cured polymer region exhibits a high loss at near-infrared wavelengths, the spectrum of the reflection from the polymer cavity is so weak as to be negligible. The interference mechanism in the proposed AG-FFPI is based on the low-finesse air-gap F-P cavity [6] and interference fringes can be measured experimentally by an optical spectrum analyzer (OSA), and used to sense the surrounding T. Fig. 2 shows the reflection spectra of the various air-gaps of AG-FFPIs at 25 °C. In this figure, d is length of the air-gap. The spectral fringes demonstrate that a longer F-P cavity has a poorer fringe visibility and a denser interference pattern in a given range of wavelengths. It is because of the light travels through a longer air-gap cavity, the larger size of the optical beam that undergoes the second reflection from the divergence of the light exiting from the single mode fiber, making interference pattern weaker. Fig. 2 also reveals that quasi-sinusoidal interference patterns over a very wide range of wavelengths can be obtained from fabricated air-gaps of various lengths. The measured fringe spacing is consistent with the relation, $\Delta\lambda_{\mathrm{m}} \sim \lambda_{\mathrm{m}}\lambda_{\mathrm{m+1}}/(2d)$ where m is an integer and λ_{m} and $\lambda_{\mathrm{m+1}}$ the central wavelengths of the two valleys adjacent to the m^{th} valley in the spectrum. Fig. 2(e) shows the NOA65 filled-length of the proposed polymer-filled AG-FFPI with HCF of D = 50 μm as a function of the duration of capillary action at different filling temperature. In the fabrication, we can control the remained air gap of the sensor by estimating the duration of capillary action based on the results of Fig. 2(e).

III. Results and Discussion

Owing to the high thermal expansion coefficient of the polymer NOA65, the proposed polymer-filled AG-FFPI is employed to measure the surrounding T, with the purpose of evaluating the effectiveness of the sensor. The device is placed on a TE cooler (Resolution: 0.1 °C) inside a closed space as T is increased from 25 °C to 70 °C. Fig. 3(a) and (b) plot the shifts of the interference dip of the proposed sensors as the T varies, with the air-gaps of about $d = 20$ μm and $d = 70$ μm, respectively. Insets display the micrograph of the HCF endface that is filled with NOA65. The micrographs reveal that NOA65 filled a section of the HCF endfaces, forming a flat-convex air-gap F-P cavity between SMF and the edge of the polymer. The concave surface of the monomer is formed because the adhesive force between the HCF and the monomer exceeds the intermolecular forces in the monomer NOA65 itself. The experimental wavelength shift (around $\lambda = 1550$ nm) and sensitivities are highly significant with a maximum sensitivity of -1.7 nm/°C. This sensitivity is almost 28 times that of the conventional LPG ($\sim +0.06$ nm/°C) because the thermal expansion coefficient of the NOA65 is 2.25×10^{-4} °C^{-1} [12], which is much greater than that of silica fiber ($\sim 5.5 \times 10^{-7}$ °C^{-1}). The air-gap F-P cavity is composed of the

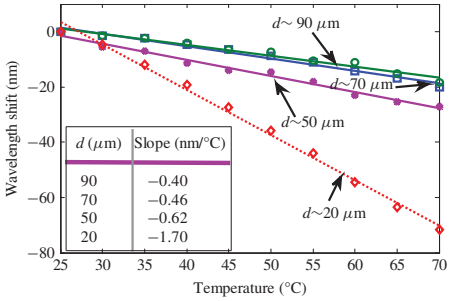

Fig. 4. Experimental temperature sensitivities of polymer-filled AG-FFPIs with different air-gaps, d.

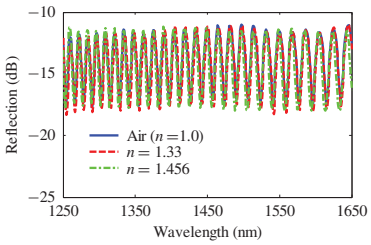

Fig. 5. Interference spectra of proposed device with air-gap d ~70 μm with various refractive indices of surroundings.

rigid silica edge of the SMF and another edge of the elastic polymer (NOA65). The force that is generated by the thermal expansion that acts mainly on the side of the elastic polymer and changes the air-gap width (Δd) of the cavity. The Δd and wavelength shifts of the m^{th} interference dip ($\Delta\lambda_m$) at the specific m^{th} interference fringe (λ_m) satisfy the relation [4]

$$\frac{\Delta d}{d} = \frac{\Delta\lambda_m}{\lambda_m}. \tag{1}$$

Fig. 4 plots the temperature sensitivity of the proposed AG-FFPIs with different lengths of air-gap. Clearly, the best sensitivity are approximately -1.7 nm/°C obtained when $d =$ 20 μm. Herein, the negative sensitivity of the proposed sensor means that the polymer section is expanded by the thermal effect that reduces the length of the air-gap (that means the Δd is negative), causing the wavelength to shift to the short wavelength side ($\Delta\lambda_m$ is negative). The ratio $\Delta d/d$ determines the shift in the fringe dips. According to Eq. (1), a smaller air-gap d is associated with a larger $\Delta\lambda_m$ at the same T and same Δd caused by same thermal expansion of the polymer. Hence, a shorter d is more sensitive and a poorer result is obtained as d increases. The results show the consistency of inversely proportional relation in the inset of Fig. 4. However, there might be some other minor factors affect the accuracy of measurement, e.g. the amount of the air remained in the air-gap, and the UV cured parameters of NOA65 in the sensor.

The interference spectra are dominated by the air-gap of F-P cavity since the measured fringe spacing depends only on the air-gap. The cavity of the polymer is a region of high loss within the measured range of wavelengths and is long enough to make the reflection by the end of the polymer negligible. Fig. 5 also demonstrates that the interference patterns and spectral intensity are barely changed by immersing the sensor heads in different surrounding liquids. Notably, the proposed device is a highly stable and a permanent structure that yields almost the same results even after several months' measurements. It is also robust and ultra-compact, and so can be used as the miniature head of a sensor that has a size of several tens of micrometers. Additionally, the ease of fabrication and lack of need for alignment are favorable characteristics of a fiber interferometer or photonic device in sensing applications.

IV. Conclusion

This work proposes a novel polymer-filled AG-FFPI and utilizes it to measure surrounding T with high sensitivity. Polymer-filled AG-FFPIs with air-gaps of several lengths were fabricated successfully. Measurements reveal that a smaller air-gap is associated with higher T sensitivity; a sensitivity of -1.7 nm/°C is achieved when the air-gap is about 20 μm. The wavelength shift is equivalent to a measured change in cavity length of -21.9 nm/°C. The developed device has very favorable characteristics and numerous advantages. We believe that it can be further developed into a state-of-the-art of hollow core-based fiber device in which NOA65 is mixed with other materials, such as chiral/nematic liquid crystals or other bio-fluids, to give it a wide range of applications.

References

[1] D.-H. Kim, J.-W. Park, H.-K. Kang, C.-S. Hong, and C.-G. Kim, "Measuring dynamic strain of structures using a gold-deposited extrinsic Fabry–Pérot interferometer," *Smart Mater. Struct.*, vol. 12, no. 1, pp. 1–5, 2003.

[2] J. Wang, B. Dong, E. Lally, J. Gong, M. Han, and A. Wang, "Multiplexed high temperature sensing with sapphire fiber air gap-based extrinsic Fabry–Pérot interferometers," *Opt. Lett.*, vol. 35, no. 5, pp. 619–621, 2010.

[3] C.-L. Lee, W.-Y. Hong, H.-J. Hsieh, and Z.-Y. Weng, "Air gap fiber Fabry–Pérot interferometer for highly sensitive micro-airflow sensing," *IEEE Photon. Technol. Lett.*, vol. 23, no. 13, pp. 905–907, Jul. 1, 2011.

[4] T. Wei, Y. Han, Y. Li, H.-L. Tsai, and H. Xiao, "Temperature-insensitive miniaturized fiber inline Fabry–Pérot interferometer for highly sensitive refractive index measurement," *Opt. Express*, vol. 16, no. 8, pp. 5764–5769, 2008.

[5] Y.-J. Rao, M. Deng, D.-W. Duan, X.-C. Yang, T. Zhu, and G.-H. Cheng, "Micro Fabry–Pérot interferometers in silica fibers machined by femtosecond laser," *Opt. Express*, vol. 15, no. 21, pp. 14123–14128, 2007.

[6] D. W. Kim, F. Shen, X. Chen, and A. Wang, "Simultaneous measurement of refractive index and temperature based on a reflection-mode long-period grating and an intrinsic Fabry–Pérot interferometer sensor," *Opt. Lett.*, vol. 30, no. 22, pp. 3000–3002, Nov. 2005.

[7] X. Chen, F. Shen, Z. Wang, Z. Huang, and A. Wang, "Micro-air-gap based intrinsic Fabry–Pérot interferometric fiber-optic sensor," *Appl. Opt.*, vol. 45, no. 30, pp. 7760–7766, Oct. 2006.

[8] C.-L. Lee, W. F. Liu, Z. Y. Weng, and F. C. Hu, "Hybrid AG-FFPI/RLPFG for simultaneously sensing refractive index and temperature," *IEEE Photon. Technol. Lett.*, vol. 23, no. 17, pp. 1231–1233, Sep. 1, 2011.

[9] H. Y. Choi, K. S. Park, S. J. Park, U.-C. Paek, B. H. Lee, and E. S. Choi, "Miniature fiber-optic high temperature sensor based on a hybrid structured Fabry–Pérot interferometer," *Opt. Lett.*, vol. 33, no. 21, pp. 2455–2457, Nov. 2008.

[10] J. Villatoro, V. Finazzi, G. Coviello, and V. Pruneri, "Photonic-crystal-fiber-enabled micro-Fabry–Pérot interferometer," *Opt. Lett.*, vol. 34, no. 16, pp. 2441–2443, Aug. 2009.

[11] R. Benmouna and B. Benyoucef, "Thermophysical and thermomechanical properties of Norland optical adhesives and liquid crystal composites," *J. Appl. Poly. Sci.*, vol. 108, no. 6, pp. 4072–4079, Mar. 2008.

[12] K. R. Sohn and G.-D. Peng, "Mechanically formed loss-tunable long-period fiber gratings realized on the periodic arrayed metal wires," *Opt. Commun.*, vol. 278, pp. 77–80, Jun. 2007.